



HAL
open science

Non-isocyanate Polyurethane Foams based on Six-membered cyclic Carbonates

Guilhem Coste, Dimitri Berne, Vincent Ladmiral, Claire Negrell, Sylvain
Caillol

► **To cite this version:**

Guilhem Coste, Dimitri Berne, Vincent Ladmiral, Claire Negrell, Sylvain Caillol. Non-isocyanate Polyurethane Foams based on Six-membered cyclic Carbonates. *European Polymer Journal*, 2022, 176, pp.111392. 10.1016/j.eurpolymj.2022.111392 . hal-03719091

HAL Id: hal-03719091

<https://hal.science/hal-03719091>

Submitted on 10 Jul 2022

HAL is a multi-disciplinary open access archive for the deposit and dissemination of scientific research documents, whether they are published or not. The documents may come from teaching and research institutions in France or abroad, or from public or private research centers.

L'archive ouverte pluridisciplinaire **HAL**, est destinée au dépôt et à la diffusion de documents scientifiques de niveau recherche, publiés ou non, émanant des établissements d'enseignement et de recherche français ou étrangers, des laboratoires publics ou privés.

Non-isocyanate Polyurethane Foams based on Six-membered cyclic Carbonates

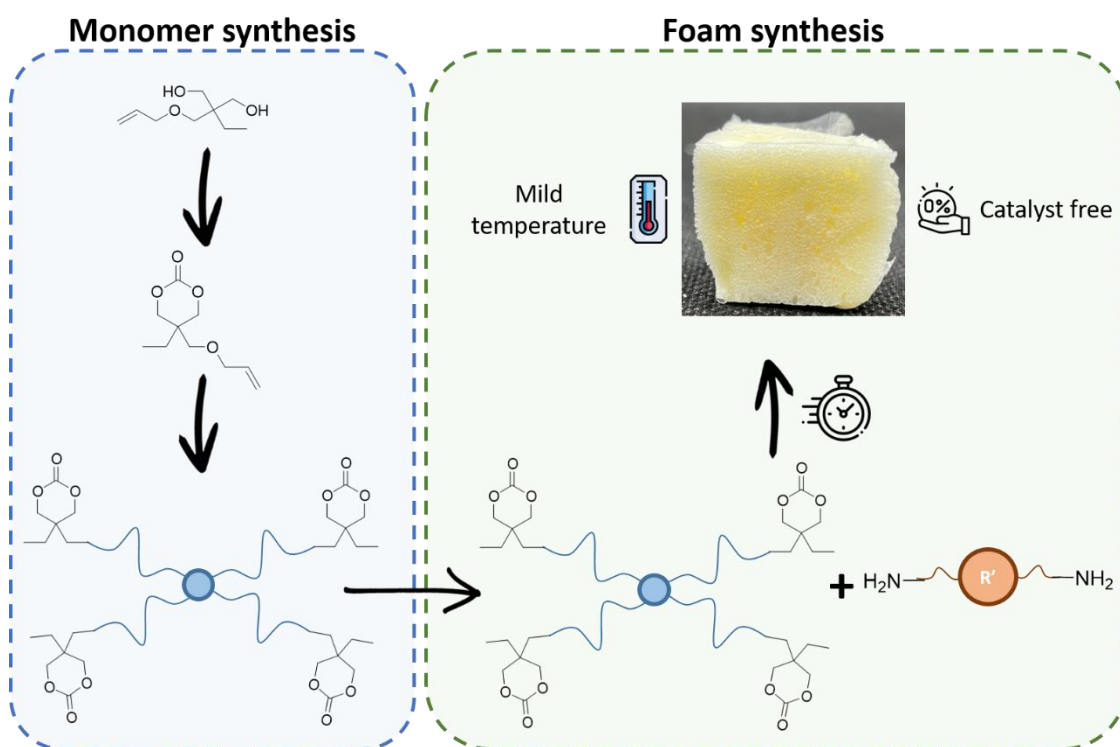
Guilhem Coste^a, Dimitri Berne^a, Vincent Ladmiral^a, Claire Negrell^a, Sylvain Caillol^a *.

*Corresponding author

^a ICGM, Univ Montpellier, CNRS, ENSCM, Montpellier, France

† In memory of Prof Yves Pietrasanta

Graphical abstract:



Abstract:

Polyurethane foams currently dominate the global foam market. Nevertheless, the main drawback of these foams remains the use of toxic isocyanate reagents. To overcome this issue, several ways have been explored. The most promising route appears to be the aminolysis of 5-membered cyclic carbonates leading to formation of polyhydroxyurethanes (PHUs). However, the lack of reactivity of systems using C5-cyclic carbonates currently limits the application range of PHUs. Hence, this study reports the first synthesis of PHUs foams using a new tetrafunctional 6-membered cyclic carbonate (TC6). The TC6 was reacted with different diamines under catalyst-free and mild temperature conditions in presence of a chemical blowing agent. Three different amines were employed, allowing access to various foams properties. Finally, promising flexible foams have been obtained, with

interesting properties that could make them possible new candidates for applications as seating or insulation mattresses.

Keywords: Foam; Non-isocyanate polyurethane; Polyhydroxyurethane; cyclic carbonate; chemical blowing agent

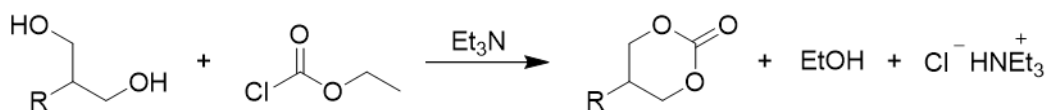
Introduction

Polyurethanes (PUs) are one of the most used polymer in the world today, their use ranges from glue for wood to binders in paint.¹ Nevertheless, the main use of these polymers remains in obtaining foams for mattresses or in insulation applications.^{2,3} Indeed, PU foams are easily accessible since PUs are directly synthesized by reaction between polyols and isocyanates. Moreover, isocyanates are known to react with air moisture which leads to the production of carbon dioxide and thus can induce foam blowing.⁴ Despite this interest in PU foams, isocyanates have long been targeted by REACH regulation and their use should be limited in the future due to their toxicity.^{5,6} Therefore, Non-Isocyanate Polyurethane (NIPU) foams represent an attractive subject due to the evolution of legislation relating to polyurethanes (PU). Thus, industrial and academic research has recently focused on this topic.

To face this PU challenge different alternatives have been developed.^{7,8} The most promising route is the step-growth copolymerization of amines with 5-membered cyclic carbonates. This route leads to PolyHydroxyUrethane (PHU) and has been extensively studied by different research groups including our team.⁹⁻¹⁷ Nevertheless, despite the advantage of the non-toxicity of the carbonate, this method has certain drawbacks. Indeed, the reactivity of the aminolysis of 5-membered cyclic carbonate is lower than that of the reaction between alcohol and isocyanate. Hence, at room temperature, PU foams can be obtained within few hours whereas in the same conditions PHU foams required at least two curing days.¹⁸⁻²⁰ Therefore, the low reactivity of PHUs synthesis limits their use for the synthesis of low density foams because the curing must be fast enough to trap the gas. Thus, in order to obtain PHUs with curing times comparable to those of PU, different ways have been explored. First, the use of catalysts has been investigated by Blain *et al.* and Lambeth *et al.*^{21,22} It was demonstrated that cyclohexylphenyl thiourea or triazabicyclodecene were the most efficient and easily available catalysts. Nevertheless, even with the use of catalysts, the aminolysis of cyclic carbonates required too long curing times. Another strategy was to develop cyclic carbonate containing activating neighboring groups (*e.g.* electron withdrawing groups) to activate the polymerization reaction.^{13,23} Only a few activating groups have an effect on the reactivity, but not enough to reduce curing times sufficiently for foams. Furthermore, larger cyclic carbonates have been developed to study the influence of ring size on the aminolysis reactivity. Hence, six-, seven- and eight-membered cyclic carbonates have been synthesized using mainly hazardous chemicals such as triphosgene and allowed to demonstrate that carbonate reactivity increases with the ring size.^{13,24,25} These results were later confirmed by Tomita *et al.* who described C6-carbonate as 29 to 62 times more reactive than C5-carbonates equivalents when reacted with benzylamine or hexylamine in catalyst-free conditions (at temperature ranging from 30°C to 70°C in *N,N*-dimethylacetamide).²³ Moreover, dithiocarbonate compounds were also described as more reactive than usual C5-carbonates but their synthesis required carbon disulfide which is a hazardous compound limiting their industrial applications.²⁶⁻²⁸ About the synthesis of C6-carbonate, they were first developed using triphosgene which is a hazardous compound as it decomposes into phosgene during C6-carbonate synthesis.^{29,30} Nowadays, other routes were developed to produce C6-carbonate using ethyl chloroformate and 1,3-diols under mild conditions (Scheme 1).³⁰ The synthesis developed by Matsuo *et al.* have been widely used for instance to prepare various mono- or bi-functional C6-carbonates.³¹⁻³⁴ Thus, one of the most promising ways of improvement to rapidly obtain PHUs is the use of C6-membered cyclic

carbonate since their synthesis is easier than C7 or C8 cyclic carbonates. However, to the best of our knowledge, no foams have been synthesized from cyclic carbonates larger than C5. Indeed, to obtain foams, cyclic carbonate monomers with functionality higher than 2 is needed. Hence, neither any multi-functional C6-carbonate nor any C6-PHU foam have been reported in the literature. Therefore, in the present study, we aimed at developing the first PHU foams synthesized from a novel multi-functional C6-membered cyclic carbonate. Concerning the source of gas required for the synthesis of foam, as for the usual C5 carbonates, the aminolysis of the C6 carbonates has the disadvantage of not producing gas directly. Thus, an external source of gas is required to blow PHU foam and that is why numerous external blowing agent have been developed. Our group recently published a review listing the different blowing agents reported in the literature.⁴ Two kinds of blowing agent can be used, either chemical or physical. Most of the C5-cyclic carbonates foams were blown by physical blowing agent.^{35,36} Nevertheless, chemical blowing agents such as the Pearson reaction or rearrangement reactions could also be used since they can be incorporated into the polymer matrix.³⁷⁻⁴⁰

Hence, in the aim to develop new C6-cyclic carbonate foams, we first developed a new tetrafunctional C6-cyclic carbonate monomer. In order to demonstrate the high reactivity of this monomer, gel time measurements were carried out with different amines. In this study, polymethylhydroxysiloxane (PMHS) was chosen as blowing agent because reactivity of both C6-cyclic carbonate and PMHS with amines were concomitant, allowing to obtain homogeneity during foam expansion. Finally, the chemical and physical properties of these catalyst-free PHU foams were evaluated according to the amine structure and respective application were proposed.



Scheme 1: Phosgene-free route synthesis of a 6-membered cyclic carbonate

Material and method

1) Material

Trimethylolpropane allyl ether (100%), Ethyl chloroformate (97%), Pentaerythritol tetrakis(3-mercaptopropionate) (PETMP, 95%), *m*-Xylylenediamine (MXDA, 99%), Triethylamine (99.5%), Azobis isobutyronitrile (AIBN, 98%), polymethylhydroxysiloxane (PMHS, $M_n=2300\text{g}\cdot\text{mol}^{-1}$) were purchased from Sigma-Aldrich (Darmstadt Germany). Isophoronediamine (cis- and trans- mixture, IPDA, 99.5%), Cadaverine (98%) were bought from TCI EUROPE N.V (Zwijndrecht, Belgium). The organic solvents, THF and 1,4-dioxane were purchased from VWR International S.A.S (Fontenay-sous-Bois, France). The additives Tegomer B 8993 and was kindly provided by Evonik (Amsterdam, Netherlands). The NMR solvent used is CDCl_3 from Eurisotop.

2) Method

Nuclear Magnetic Resonance

Proton Nuclear Magnetic Resonance (^1H NMR) analyses were carried out in deuterated chloroform (CDCl_3 , 99.50% isotopic purity) using Bruker Avance III 400 MHz NMR spectrometer at a temperature of 25 °C.

Fourier Transform Infrared Spectroscopy

Infrared (IR) spectra were recorded on a *Nicolet IS50* Fourier transform infrared spectroscopy (FTIR) spectrometer. The characteristic IR absorptions mentioned in the text are only strong bands reported in cm^{-1} .

Thermogravimetric Analyses

Thermogravimetric Analyses (TGA) were carried out using TG 209F1 apparatus (Netzsch). Approximately 10 mg of sample were placed in an alumina crucible and heated from room temperature to 800°C at a heating rate of 20 °C/min under nitrogen atmosphere (40 mL/min). A nitrogen flow was used to protect the apparatus.

Differential Scanning Calorimetry

Differential Scanning Calorimetry (DSC) analyses were carried out using a NETZSCH DSC200F3 calorimeter, which was calibrated using indium, n-octadecane, n-octane, adamantane, biphenyl, tin, bismuth and zinc standards. Nitrogen was used as purge gas. Approximately 10 mg of sample were placed in a perforated aluminum pan and the thermal properties were recorded between -150 °C and 120 °C at 20 °C/min to observe the glass transition temperature. The T_g values were measured on the second heating ramp to erase the thermal history of the polymer. All the reported temperatures are average values on three different tries.

Hardness

Shore 0 hardness for foam was measured on a durometer Shore Hardness Tester HD0 100-1 from Sauter. Samples with 0.5 cm thickness were prepared for the measurement. An average of five measurements was performed.

Gel content

Three samples from the same material, of around 20 mg each, were separately immersed in THF for 24 h. The three samples were then dried in a ventilated oven at 70°C for 24h. The gel content (GC) was calculated using equation (1), where m_2 is the mass of the dried material and m_1 is the initial mass. Reported gel content are average values of the three samples.

$$GC = \frac{m_2}{m_1} \times 100 \quad (1)$$

Scanning electron microscopy

The morphology and the internal structure of the foams were analyzed using in parallel surface to the rise direction of NIPU foam by scanning electron microscopy (SEM). A FEI Quanta 200 FEG was used to obtained foam images.

Rheological experiments

The gelation times were measured using a Thermo Fisher HAAKE MARS rheometer with a plate–plate geometry with a diameter of 25 mm. The gelation times were analyzed by observing the crossover of the storage modulus (G') and loss modulus (G'') during an oscillatory experiment at 1 Hz, 50 °C and 2% of deformation, according to the previously determined linear domain. Compression tests were carried out using this apparatus since it allowed higher shift compare to DMA. The maximum force is higher 60 N vs 50 N for the DMA. The samples were compressed at 50% of their height for the foam with MXDA and cadaverine. The compression was increased to 70% with IPDA foam. The sample were compressed in 30 seconds. The obtained normal force was divided by the surface of the sample to obtain the measurement in Pascal.

Titration of the amine equivalent weight of amine by ¹H NMR

The Amine Equivalent Weight (AEW) is the amount of product needed for one equivalent of reactive amine function. It was determined by ¹H NMR using and internal standard (benzophenone). Known masses of product and benzophenone were poured into a NMR tube and 550 μL of CDCl₃ were added. The AEW was determined using equation (2) by comparing the integration value of the signals assigned to the benzophenone protons (7.5-7.8 ppm) with the integration of the signals arising from

amine moiety protons (4.33 ppm with MXDA, 2.61 ppm with cadaverine and 2.57 plus 2.60, 2.41 for IPDA).

$$AEW = \frac{\int PhCOCPH \times H_{amine}}{\int amine \times H_{PhCOCPH}} \times \frac{m_{amine}}{m_{PhCOCPH}} \times M_{PhCOCPH} \quad (2)$$

$\int_{PhCOCPH}$: integration of the signal from benzophenone protons; \int_{amine} : integration of the signals from protons in α the amine function; H_{amine} : number of protons in α of the amine function; $H_{PhCOCPH}$: number of benzophenone protons; m_{amine} : amine mass; $m_{PhCOCPH}$: benzophenone mass; $M_{PhCOCPH}$: benzophenone molecular weight.

Titration of the carbonate equivalent weight by 1H NMR

The Carbonate Equivalent Weight (CEW) is the amount of product needed for one equivalent of reactive cyclic carbonate or thiocarbonate function. It was determined by 1H NMR using an internal standard (benzophenone). Known masses of product and benzophenone were poured into a NMR tube and 550 μ L of $CDCl_3$ were added. The CEW was determined using equation (3) by comparing the integration value of the signals assigned to the benzophenone protons (7.5-7.8 ppm) with the integration of the signals arising from cyclic carbonate (4.94 ppm for TC6).

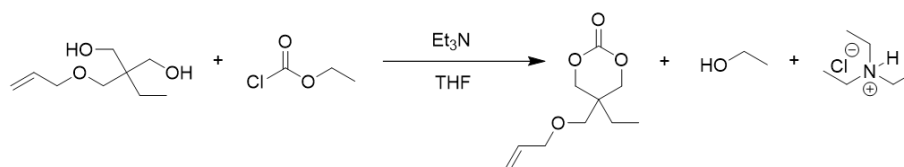
$$CEW = \frac{\int PhCOCPH \times H_{carbonate}}{\int carbonate \times H_{PhCOCPH}} \times \frac{m_{carbonate}}{m_{PhCOCPH}} \times M_{PhCOCPH} \quad (3)$$

$\int_{PhCOCPH}$: integration of the signal from benzophenone protons; $\int_{carbonate}$: integration of the signals from protons in α of the carbonate function; $H_{carbonate}$: number of protons in α of the carbonate function; $H_{PhCOCPH}$: number of benzophenone protons; $m_{carbonate}$: product mass; $m_{PhCOCPH}$: benzophenone mass; $M_{PhCOCPH}$: benzophenone molecular weight.

3) Synthesis

Monomer synthesis

Synthesis of 5-((allyloxy)methyl)-5-ethyl-1,3-dioxan-2-one (MC6)



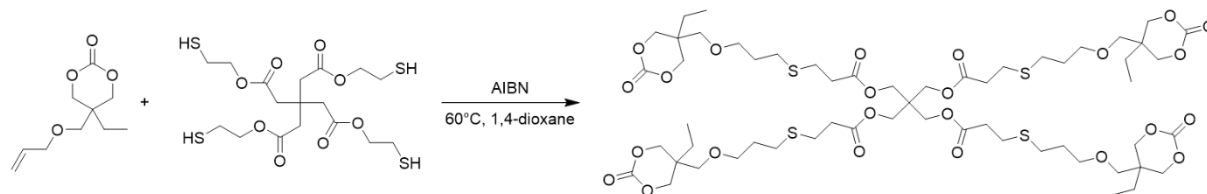
Scheme 2: MC6 synthesis

This protocol was reproduced from the publication of V. Besse *et al.*²⁸ In a two-neck round-bottom flask (1 L), trimethylolpropane allyl ether (43.6 g, 250 mmol, 1 eq.) was dissolved in dry THF. Ethyl chloroformate (78.7 g, 725 mmol, 2.9 eq.) was added and the solution was mixed for ten minutes. Then, triethylamine (75.9 g, 750 mmol, 3 eq.) was added drop by drop at 0 °C for 1 h. The reaction mixture was then stirred at room temperature for 24 h and was filtered prior to its concentration under vacuum. Then, the crude product was diluted with ethyl acetate and washed two times with aqueous hydrochloric acid (0.5 mol) and two times with saturated $NaHCO_3$ solution and finally with brine two times. The organic solution was dried with $MgSO_4$ and under vacuum to obtain MC6 as a colorless liquid (42.4 g) with 85 % of yield.

1H NMR (Figure S11) (400 MHz, $CDCl_3$, ppm) δ : 0.92-0.96 (t, 3H, $^3J_{H-H} = 7.6$ Hz, CH_3-CH_2), 1.53-1.58 (q, 2H, $^3J_{H-H} = 7.6$ Hz, CH_3-CH_2), 3.42 (s, 2H, O- CH_2 -C), 3.99-4.01 (dt, 2H, $^3J_{H-H} = 5.6$ Hz, $^4J_{H-H} = 1.4$ Hz, $CH_2=CH_2-CH_2-O$), 4.15-4.17 (d, 2H, $^2J_{H-H} = 10.9$ Hz, C- CH_2 -O-C=O), 4.35-4.37 (d, 2H, $^2J_{H-H} = 10.9$ Hz, C- CH_2 -O-C=O), 5.21-5.22 (ddd, 1H, $^2J_{H-H} = 2.9$ Hz, $J^3 = 10.4$ Hz, $J^4 = 1.3$ Hz, $CH_2=CH-CH_2-O$), 5.26-5.31

(ddd, 1H, $^2J_{H-H} = 2.9$ Hz, $^3J_{H-H} = 17.2$ Hz, $^4J_{H-H} = 1.4$ Hz, $CH_2=CH-CH_2-O$), 5.83-5.93 (ddt, $^3J_{H-H} = 17.2$, 10.4, 5.6 Hz, $CH_2=CH-CH_2-O$).

Synthesis of 2,2-bis(((3-((3-((5-ethyl-2-oxo-1,3-dioxan-5-yl)methoxy)propyl)thio)propanoyl)oxy)methyl) propane -1,3-diyl bis(3-((3-((5-ethyl-2-oxo-1,3-dioxan-5-yl)methoxy)propyl)thio)propanoate) (TC6)



Scheme 3: TC6 synthesis

In a round-bottom flask, MC6 (40.05 g, 200 mmol, 1 eq.) was diluted in 1,4-dioxane (80 mL) with AIBN (1.64 g, 20.0 mmol, 0.05 eq.) Then the reaction was placed under argon atmosphere and pentaerythritol tetrakis(3-mercaptopropionate) (PETMP, 24.43 g, 50 mmol, 0.25 eq.) was introduced via a syringe. The mixture was then stirred at 60 °C for 16 h until no more typical allyl double-bond signals were detected in proton NMR. The solvent was then evaporated under reduced pressure and the crude product solubilized in ethyl acetate prior to be washed two times with water. Organic phases were collected, dried over magnesium sulfate, and concentrated under vacuum to obtain the pure product as a yellowish viscous liquid (56 g) with 87 % of yield.

1H NMR (Figure SI2) (400 MHz, $CDCl_3$, ppm) δ : 0.92-0.96 (t, 3H, $^3J_{H-H} = 7.6$ Hz, CH_3-CH_2), 1.50-1.57 (q, 2H, $^3J_{H-H} = 7.6$ Hz, CH_3-CH_2), 1.83-1.90 (m, 2H, $S-CH_2-CH_2-CH_2-O$), 2.60-2.72 (m, 4 H, CH_2-S-CH_2), 2.77-2.80 (t, 2H, $^3J_{H-H} = 6.9$ Hz, $O=C-CH_2-CH_2-S$), 3.44 (s, 2H, CH_2-O-CH_2-C), 3.53-3.56 (t, 2H, $^3J_{H-H} = 6.0$ Hz, CH_2-CH_2-O), 4.15-4.18 (d, 2H, $^2J_{H-H} = 10.9$ Hz, $C-CH_2-O-C-O$), 4.20 (s, 2H, $C-CH_2-O-C=O$), 4.35-4.37 (d, 2H, $^2J_{H-H} = 10.9$ Hz, $C-CH_2-O-C-O$).

^{13}C NMR (Figure SI3) (400 MHz, $CDCl_3$, ppm) δ : 7.5 (CH_3-CH_2), 23.5 (CH_3-CH_2), 26.7 ($O=C-CH_2-CH_2-S$), 28.6 ($S-CH_2-CH_2-CH_2-O$), 29.3 ($S-CH_2-CH_2-CH_2-O$), 34.6 ($O=C-CH_2-CH_2-S$), 35.4 (CH_3-CH_2-C), 45.1 ($C-CH_2-O-C=O$), 60.8 ($C-CH_2-O-C=O$), 69.4 (CH_2-O-CH_2-C), 69.9 ($S-CH_2-CH_2-CH_2-O$), 72.9 ($C-CH_2-O-C-O$), 148.6 ($O-C-O$), 169.4 ($CH_2-O-C=O$).

Figure SI4 presented the 2D NMR.

General procedure of foam synthesis

Materials were synthesized with a cyclic carbonate molar/amine ratio of 1/1. The amine and carbonate masses were calculated with the equation (5) and (6), respectively, where $n_{\text{carbonate}}$ and n_{amine} are the number of moles of cyclic carbonate or amine, and AEW is the amine equivalent weight and CEW is the carbonate equivalent weight. The formulations of NIPUs networks were calculated from 1 equivalent of carbonate, 1 equivalent of amine. An excess of amine function was then used to react with PMHS to produce gas, one amine function reacts with one siloxane function (32 in PHMS). The mass targeted for each formulation is approximately of 10g. First, the TC6 plus the surfactant were placed in the plastic beaker and mechanically mixed for 2 minutes. Then the blowing agent was added to the mixture and stirred mechanically 30 seconds. Finally, the amine is quickly added to the mixture and stirred mechanically for 30 seconds. The formulation is then transferred in a silicon mold and heated overnight at 50°C. Then, 2 hours at 120°C post curing is applied to the foams. This curing has been defined as optimal since it showed no residual peak in DSC after treatment. All structural additives were used following the technical data sheet of the suppliers.

Table 1: AEW and CEW of the monomers

	Cadaverine	MXDA	IPDA	Priamine®	TC6
CEW (g.eq ⁻¹)	-	-	-	-	342
AEW (g.eq ⁻¹)	51.1	68.1	85.2	309	-

Result and discussion

Foam synthesis

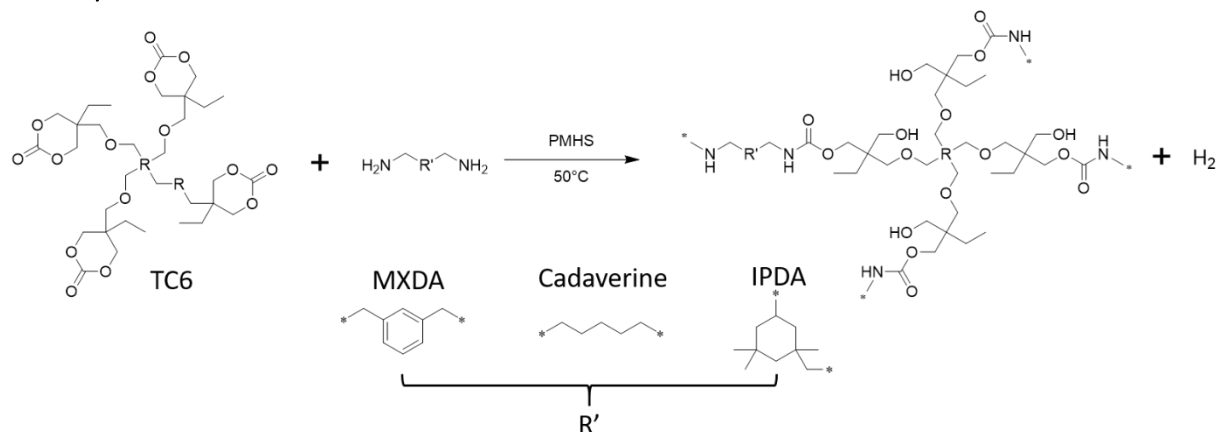


Figure 4: General synthesis of C6 foams

In order to perform catalyst-free foam synthesis at relatively mild temperature, the addition of an amine on a C6-cyclic carbonate was selected as the polymerization reaction. The formation of a crosslinked network is required to obtain foams hence at least one of the monomers (amine or cyclic carbonate) should possess a functionality strictly above two. There is no many commercial trifunctional amines (except tris(2-aminoethyl)amine or Jeffamine® Triamines) and easily accessible di-C6-cyclic carbonates are usually solid which complicates foam formulation. In order to overcome these obstacles, an innovative cyclic tetra-C6 carbonate (TC6) monomer has been synthesized.

Based on the work of Besse *et al.*, a C6-cyclic carbonate bearing an allyl function was reproduced (Figure S1). Then, by performing thiol-ene addition of this C6-cyclic carbonate on pentaerythritol tetrakis(3-mercaptopropionate) (PETMP) in presence of AIBN at 60 °C for 16h in dioxane, TC6 was obtained in good yield. The TC6 monomer was characterized by ¹H, ¹³C and ¹H-¹³C HSQC NMR (Figure S2-4) and the carbonate equivalent weight (CEW) of this TC6 has been determined by ¹H-NMR using the Equation (3). The CEW of 342 g.eq⁻¹ confirmed that TC6 functionality (3.8) makes it a crosslinking monomer (Table 1). The amine hydrogen equivalent weights (AEW) of the different amines were also evaluated by ¹H-NMR to precisely determine the required ratio of amine and cyclic carbonate for each foam formulation.

The formation rate of the crosslinked network was evaluated according to the reaction between TC6 and various diamines without blowing agent. We have selected Priamine®, cadaverine, *m*-xylylenediamine (MXDA) and isophorone diamine (IPDA). The curing rate of the different formulations was evaluated by performing rheological kinetics on the cyclic carbonate/amine mixtures at 50 °C (Figure 5). Reactivity order corresponds to the one expected from literature: cadaverine > MXDA > IPDA.⁴³ Foams were obtained which means that aminolysis of both cyclic carbonates and PMHS had approximately the same rate of reaction. By opposition, no gel point was observed after 2 hours at 50 °C for the formulation based on Priamine®. Indeed, this amine has long aliphatic chains that confer steric hindrance, associated with a lower reactivity. This observation

explains why a sticky material was obtained with Priamine®, compare to others foams with other diamines. Thus, for the following investigations Priamine® was not used.

These rheological kinetic studies highlighted the potential of C6-monomer for catalyst-free foam synthesis compared to C5-monomer. Indeed, the curing time required for these C6-materials was lower than that of C5-cyclic carbonates. To demonstrate the higher reactivity of the C6-cyclic carbonate, a formulation containing trimethylolpropane tricyclic carbonate (TMPTC5) was reacted with cadaverine in the same conditions, *e.g.* catalyst-free at 50°C (Figure S15). The gel time was not reached in 3 hours with TMPTC5 whereas the gel time with the TC6 was 347s. Thus, this confirmed previous results mentioned in the introduction.²⁴⁻²⁶ The influence of the amine structure on chemical and physical foam properties were evaluated in the following parts.

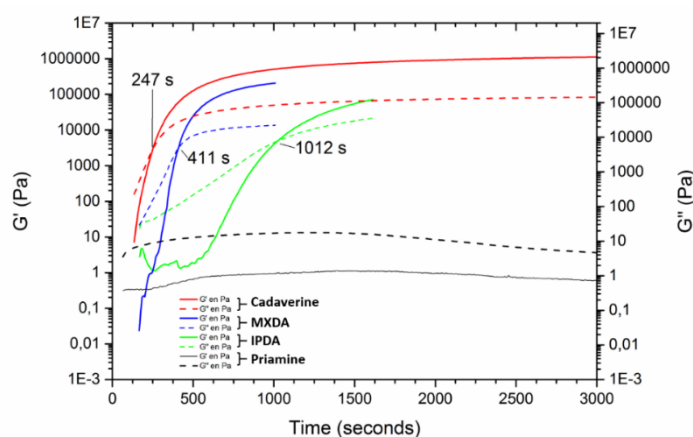


Figure 5: Gel time of the different formulations

During foam synthesis, on one hand, the aminolysis of C6-cyclic carbonate yielded a hydroxyurethane which allowed crosslinking reaction. On the other hand, the formation of dihydrogen from the addition of an amine onto hydrosiloxane allowed the blowing reaction. In this study, PMHS was used as the source of hydrosiloxane. This blowing agent has been previously used by Stefani *et al.* in epoxy foams and by our group for the synthesis of the first C5-PHU foams.^{37,43} Usually, catalyst is required to obtain PHUs foams.³⁷ The use of C6 highly reactive carbonate allowed to avoid the use of any catalyst.

The foams were prepared with cadaverine, MXDA or IPDA (Table 2). The different diamine structures enabled accessing to a large range of foam properties. Foams were synthesized by using a ratio of 1.5/1 of amine/cyclic carbonate and 5% weight of Polymethylhydrosiloxane was used. The final network should theoretically be composed of two hydroxyl-urethane functions for one silazane group (covalent bond between silicon and nitrogen). The final shape of the foams were obtained after 4 hours at 50°C. Nevertheless in order to have a fully inert material for further thermal analysis, a post curing of 2 hours at 120°C was performed. These foams were then chemically and physically analyzed (Table 2 and 3).

The formation of a crosslinked network was assessed by performing gel content and by FTIR spectrometry. High gel contents were obtained for the three formulations confirming a high conversion of the reactive functions (Table 2). From FTIR spectra, cyclic carbonate groups are characterized by a band at 1735 cm^{-1} corresponding to C=O elongation and the amine functions are characterized by a band around 1595 cm^{-1} (1598 cm^{-1} for cadaverine and IPDA and 1589 cm^{-1} for MXDA) associated to the N-H bond plan deformation and bands around 3280 cm^{-1} and 3355 cm^{-1} (3285 and 3358 cm^{-1} for cadaverine, 3279 and 3352 cm^{-1} for IPDA and 3280 and 3361 cm^{-1} for MXDA) associated to N-H bond elongation. These characteristic bands are no longer detectable in foam

analyses, instead the presence of a band around 1695 cm^{-1} (1697 cm^{-1} for MXDA and IPDA and 1694 cm^{-1} for cadaverine) corresponding to C=O bond elongation indicates the formation of urethane bond (Figure 5). More specifically hydroxyl-urethane bonds are formed during this synthesis. This result was confirmed by the presence of a large band at 3320 cm^{-1} corresponding to O-H elongation. These analyses confirmed the formation of highly crosslinked PHU.

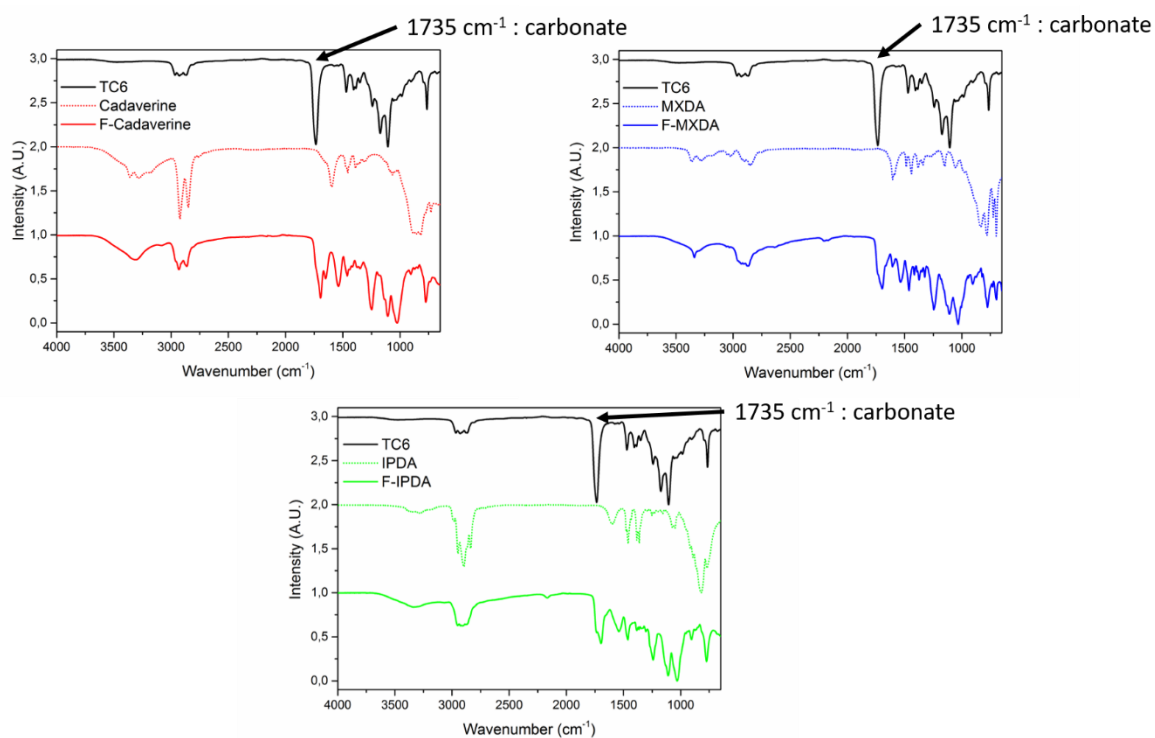


Figure 5: IR spectra of the TC6, diamines and foams.

Material properties

Four different foams were obtained after thermal curing. It can be first noticed that the foams based on MXDA and cadaverine appeared to be more flexible than IPDA one which was more rigid and brittle. This could potentially lead to the destruction of the IPDA foam under compression and limits its range of application.

The thermal behavior of the synthesized foams in presence of additive was evaluated by TGA (Figure SI6) and DSC (Figure SI7) analyses. The glass transition followed the expected trend, cadaverine foam exhibited the lower T_g ($7\text{ }^\circ\text{C}$) followed by MXDA foam ($15\text{ }^\circ\text{C}$) and IPDA foam ($27\text{ }^\circ\text{C}$).^{41,44} Hence, the presence of carbon cycle on amine structure appeared to reduce chain mobility and therefore increase glass transition temperature. The higher T_g obtained for IPDA compared to MXDA foams could be linked to the α -position of the amine on the aliphatic ring. Indeed, with MXDA there is a sp^2 carbon between the amine and the ring providing more flexibility to the polymer matrix compared to IPDA. TGA analyses were also performed to assess thermal foam stability. The different foams exhibited a $T_{d\ 1\%}$ between $100\text{ }^\circ\text{C}$ and $160\text{ }^\circ\text{C}$ which can be linked to the presence of residual solvent. It cannot be the amines because their boiling points are higher, respectively $178\text{ }^\circ\text{C}$ for the cadaverine and $247\text{ }^\circ\text{C}$ for MXDA and IPDA. The values are not similar because the TC6 used was synthesized using different batches. All samples were stable up to $280\text{ }^\circ\text{C}$ (less than 5% weight loss, $T_{d\ 5\%}$). The degradation occurred at the lowest temperature for cadaverine foam as this formulation contains small alkyl chains. The presence of a conjugated cycle in MXDA foam improved its thermal stability

compared to IPDA one for which the carbon cycle was only composed of alkyl bonds. The aromatic rings are known to improve the char formation, which is why the MXDA foam had higher residual mass (Figure S16). Then IPDA foam had a lower char content due to the cycloaliphatic ring. The small alkyl chains of the cadaverine led to the lowest residual mass.

Table 2: Chemical and Physical properties of C6-foams

Foam	T _{d 1%} (°C)	T _{d 5%} (°C)	T _g (°C)	GC (%)
F-MXDA	158	305	15	81
F-Cadaverine	100	274	7	80
F-IPDA	135	283	27	82

The curing of the C6-foam without catalyst was confirmed by FTIR and gel content analyses. The impact of the amine structure could be already observed on thermal behavior of the different foams. In the following sections, specific foams properties were also evaluated according to the amine structure.

Foam properties

First, the influence of the presence of an additive on foam aspect was evaluated. Usually additives play crucial role in foam synthesis since they avoid the different phenomena such as the Ostwald ripening or the cell drainage.⁴⁵ Thus, to determine the effect of the additive on these new C6 foams the MXDA formulation was prepared with and without the Tegomer B 8893 respectively called F-MXDA and F-MXDA no Add. For these two foams the same preparation protocol was followed. The effect of the additive on foam aspect could be clearly observed visually (Figure S18), the additive-free foam showed a lower and non-homogeneous expansion compared to the additive-based one. Thus, in this study, a stabilizer was required to obtain homogenous foams.

By visually comparing F-Cadaverine, F-MXDA and F-IPDA foams, it can be noticed that F-MXDA and F-Cadaverine had similar shape at the end of the curing protocol. However, the IPDA foam showed a higher expansion and an important increase of the pores size. These observations can be associated to the different gel points obtained for these formulations. Indeed, cadaverine and MXDA formulations had quite similar gel times (around 4 and 7 min respectively) compared to the IPDA one which clearly had a longer gel time (around 17 min) at 50°C. Longer reaction time led to higher expansion since the gas had more time to expand. Thus, the shape of the foam could be modified using different amine structures with a similar curing. Nevertheless, all the C6-foams had similar interconnected cells. The aspect of the foams was also visually analyzed by scanning electron microscopy (Figure 6). The SEM analysis demonstrated high homogeneity for the three foams as shown in the Figure 6. The pores size follows the expected trend. The F-IPDA had the largest pore size about 1.35 ± 0.32 mm then the cadaverine with cells size about 0.42 ± 0.19 mm and finally the MXDA foam with cells size about 0.21 ± 0.07 mm. The numbers of cells by cm³ or NCell calculated (Table 3) were coherent with the pores size. Indeed, the high number of pores by cm³ was measured for low pores size. Thus, the F-MXDA has the highest NCell about 1700 cells.cm⁻³ when the F-Cadaverine has 1300 cells.cm⁻³ and IPDA 280 cells.cm⁻³. The difference between F-MXDA and F-Cadaverine is slight because of the low pores size difference. However the F-IPDA which is characterized by the largest pores had a low NCell. For the same reasons, despite a low NCell, the IPDA foam had the lowest density with 0.17 ± 0.01 . The F-MXDA had the highest density due to the small pores despite their higher number compared to F-Cadaverine.

F-MXDA

F-Cadaverine

F-IPDA

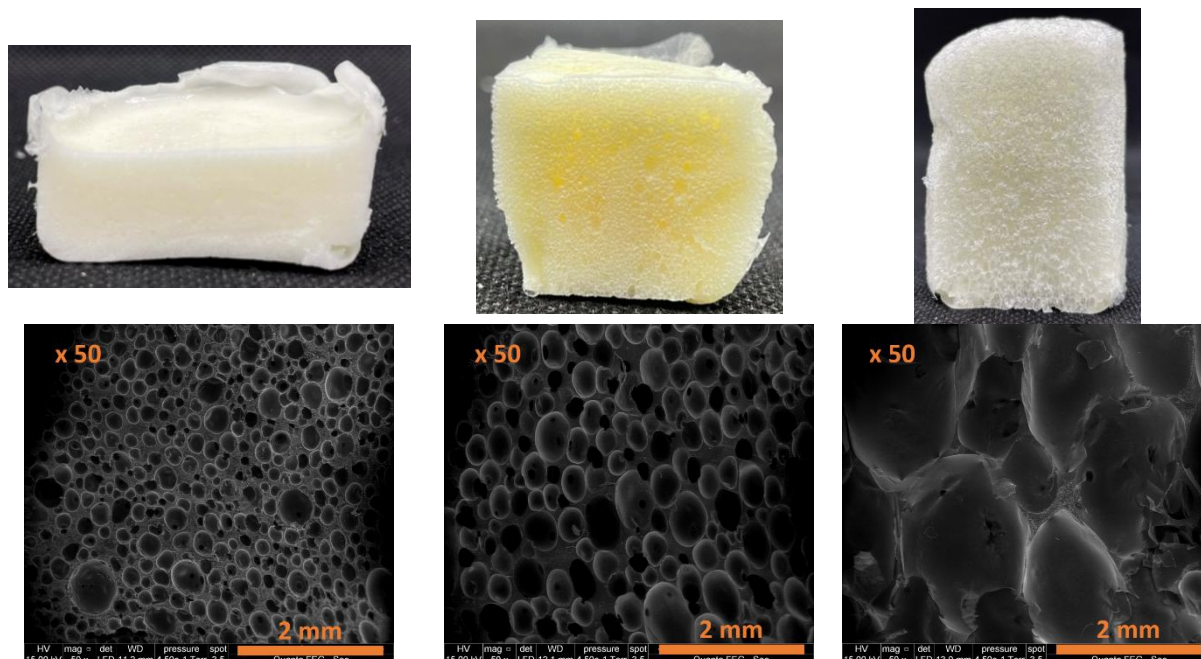


Figure 6: Optic and SEM pictures of the three different C6 foams.

Mechanical properties

After the visual characterization, the physical properties of the foam were also analyzed. First, the hardness of the foams was measured using Shore test 0 designed for foams. This test measured the hardness at the surface of the foam. A glass is the reference with hardness value at 100. The obtained results were coherent with the glass transition trend observed (Table 3). Indeed, F-MXDA and F-IPDA had higher hardness than F-Cadaverine due to their diamines structures. Moreover the IPDA foam has the highest hardness as expected since it has the highest glass transition (above 25 °C).

Table 3: Microscopic and mechanical analysis.

Foams	Cell size (mm)	ρ_a (g.cm ⁻³)	Cell density (NCell) (cells.cm ⁻³) ^a	Shore test	Stress at 50% strain (kPa) ^b
F-MXDA	0.21 ± 0.07	0.53 ± 0.06	1700	10	215
F-Cadaverine	0.42 ± 0.19	0.35 ± 0.04	1300	5	165
F-IPDA	1.35 ± 0.32	0.17 ± 0.01	280	34	140

^a a: $N_{cell} = (nM/A)3/2ps/pp$; with the number in SEM image (n, average on 3 images), magnification (M), surface area of the image (A, mm²), sample density of solid (ps) and foam density (pp). The solid density of non-foamed samples was estimated at 0.94 ± 0.07 g.cm⁻³ for the F-MXDA with, 0.87 ± 0.04 g.cm⁻³ for F-cadaverine, and 1.05 ± 0.02 g.cm⁻³ for F-IPDA. ^b at 70% strain for the F-IPDA

Compression tests have also been carried out on the different foams (Figure 7). Such analysis on foams allowed the observation of three different regions: the linear elasticity, the plateau and the densification. The first region corresponds to the strain for edge bending of the foam. The second region corresponds to the collapse due to the cells compression. And finally when all the cells are compressed and each face of the cells is in contact, this corresponds to the densification region. The densification corresponds to a high increase of the stress for a lower strain applied. Depending on the previous results, three compression regions are expected with MXDA and cadaverine. However, with the IPDA foams which is highly rigid, it is expected that the cells will be destroyed during the compression. On the plateau region the pores would be crushed down, inducing a decrease of the stress.

Compression tests presented in Figure 7 confirmed these predictions. Indeed, the different regions were well observed with the flexible foams (MXDA and cadaverine). F-MXDA and F-cadaverine respectively showed a plateau from 10% to 35% and from 14% to 40%. The slight shift in the plateau might be linked to the chemical structure of the amine. Indeed, MXDA foam contains an aromatic ring which improves the hardness as observed with the Shore test 0. Thus, the linear elasticity of the F-MXDA might be lower than the foam with cadaverine, therefore the plateau appeared quickly for MXDA compared to cadaverine foam. These foams could be potentially used as sitting mattress.

The F-IPDA foam was not compared to the two other foams because it is a rigid foam which breaks before bending (Figure 7). As the pores size is more important in F-IPDA compare to the two other foams, it was required to increase the strain range to 70% to observe the characteristic three regions. First, the linear elasticity increased quickly due to the rigidity of the foams as observed with Shore test. Then a “plateau” regime was reached. However, unlike the other foams, the stress decreased while the strain increased which is due to the cell collapse phenomena. Finally, the densification region was reached at 50% strain when all the pores were crushed. The F-IPDA sample was totally destroyed after the analysis. This foam demonstrated a specific behavior as after 22% strain the polymer matrix appeared to be already destroyed. Thus, such foam could not be used for multiple compression cycles and could rather be used as rigid insulation foam.

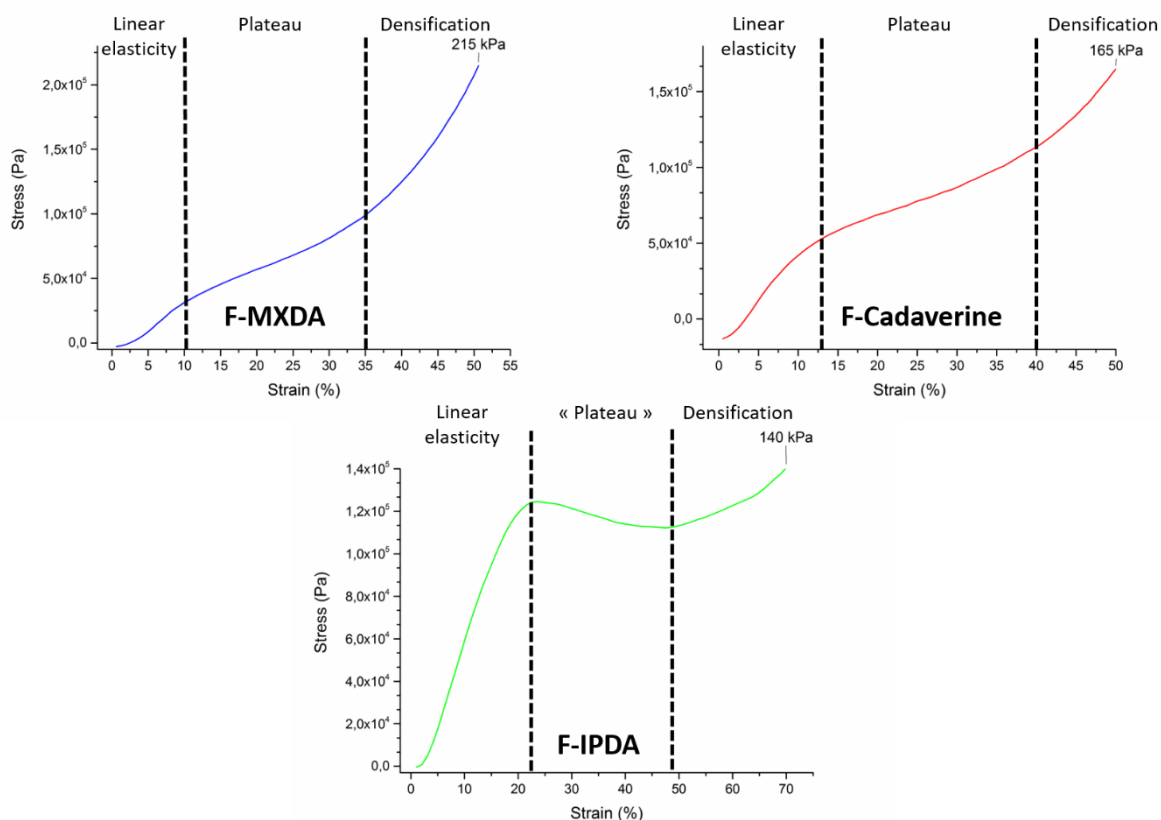


Figure 7: Compression test of the different foams.

Conclusion

In this study, the specific reactivity of C6 carbonate toward the formation of PHU was used to produce new foams. For this purpose, a new tetra-functional C6-carbonate (TC6) was synthesized and reacted with different diamines in presence of hydroxysiloxane oligomers as blowing agent. Using the higher reactivity of the C6-cyclic carbonate, the foam syntheses were performed with different amines in catalyst-free conditions and under mild conditions (4 h, 50 °C). The materials

demonstrated high gel content and carbonate conversion confirming polymer formation. Thus, the interest of C6 carbonates reactivity was demonstrated for foam application.

The structure of diamines was used to tune the foam properties. They influenced the shape, the mechanical and thermal properties of the foams. These foams have similarities with usual PU foams, which can be rigid to flexible with broad pore sizes. From SEM analyses, all the synthesized foams presented an open cell structure but the cells size depends on the amine used. Compression tests enabled to determine possible applications for the foams according to the structure of the diamine. Hence, foams using MXDA or cadaverine could be used as sitting mattress whereas IPDA foam could be used as insulation foam. Future works could be carried out on various C6-cyclic carbonates to tune the foam properties and also reach a foam synthesis at room temperature.

Acknowledgments

The authors would like to acknowledge Frédéric Fernandez from the MEA platform, Université de Montpellier, for the SEM experiments and sample preparation.

References

1. Randall, D.; Lee, S. *The Polyurethanes Book*; Randall, D.; Lee, S., Eds.; J. Wiley, **2002**.
2. Gama, N. V; Ferreira, A.; Barros-Timmons, A. Polyurethane foams: Past, present, and future. *Materials (Basel)*. **2018**, *11*, 1841–1876.
3. Wirpsza, Z. *Polyurethanes: Chemistry, Technology, and Applications*; Kemp, T. J., Ed.; E. Horwood, **1993**.
4. Coste, G.; Negrell, C.; Caillol, S. *Eur. Polym. J.* **2020**, *140*.
5. Stefanie Merenyi *REACH: Regulation (EC) No 1907/2006: Consolidated version (June 2012) with an introduction and future prospects regarding the area of Chemicals legislation*; **2012**.
6. Bello, D.; Herrick, C. A.; Smith, T. J.; Woskie, S. R.; Streicher, R. P.; Cullen, M. R.; Liu, Y.; Redlich, C. A. *Environ. Health Perspect.* **2007**, *115*, 328.
7. Khatoon, H.; Iqbal, S.; Irfan, M.; Darda, A.; Kanwar, N. *Prog. Org. Coatings* **2021**, *154*, 106124.
8. Gomez-Lopez, A.; Elizalde, F.; Calvo, I.; Sardon, H. *Chem. Commun.* **2021**, *57*, 12254.
9. Panchireddy, S.; Grignard, B.; Thomassin, J. M.; Jerome, C.; Detrembleur, C. *Polym. Chem.* **2018**, *9*, 2650.
10. Kihara, N.; Kushida, Y.; Endo, T. *J. Polym. Sci. Part A Polym. Chem.* **1996**, *34*, 2173.
11. Poussard, L.; Mariage, J.; Grignard, B.; Detrembleur, C.; Jérôme, C.; Calberg, C.; Heinrichs, B.; De Winter, J.; Gerbaux, P.; Raquez, J. M.; Bonnaud, L.; Dubois, P. *Macromolecules* **2016**, *49*, 2162.
12. Carré, C.; Ecochard, Y.; Caillol, S.; Avérous, L. *ChemSusChem* **2019**, *12*, 3410.
13. Cornille, A.; Blain, M.; Auvergne, R.; Andrioletti, B.; Boutevin, B.; Caillol, S. *Polym. Chem.* **2017**, *8*, 592.
14. Figovsky, O.; Shapovalov, L.; Leykin, A.; Birukova, O.; Potashnikova, R. *PU Mag.* **2013**, *10*, 2.
15. Nishikubo, T.; Iizawa, T.; Iida, M.; Isobe, N. *Tetrahedron Lett.* **1986**, *27*, 3741.
16. Besse, V.; Auvergne, R.; Carlotti, S.; Boutevin, G.; Otazaghine, B.; Caillol, S.; Pascault, J. P.;

- Boutevin, B. *React. Funct. Polym.* **2013**, *73*, 588.
17. Aoyagi, N.; Furusho, Y.; Endo, T. *J. Polym. Sci. Part A Polym. Chem.* **2013**, *51*, 1230.
 18. Kihara, N.; Endo, T. *J. Polym. Sci. Part A Polym. Chem.* **1993**, *31*, 2765.
 19. Cornille, A.; Guillet, C.; Benyahya, S.; Negrell, C.; Boutevin, B.; Caillol, S. *Eur. Polym. J.* **2016**, *84*, 873.
 20. Arbenz, A.; Perrin, R.; Avérous, L. *J. Polym. Environ.* **2018**, *26*, 254.
 21. Blain, M.; Jean-Gérard, L.; Auvergne, R.; Benazet, D.; Caillol, S.; Andrioletti, B. *Green Chem.* **2014**, *16*, 4286.
 22. Lambeth, R. H.; Henderson, T. *J. Polymer (Guildf)*. **2013**, *54*, 5568.
 23. Tomita, H.; Sanda, F.; Endo, T. *J. Polym. Sci. Part A Polym. Chem.* **2001**, *39*, 3678.
 24. Yuen, A.; Bossion, A.; Gómez-Bengoa, E.; Ruipérez, F.; Isik, M.; Hedrick, J. L.; Mecerreyes, D.; Yang, Y. Y.; Sardon, H. *Polym. Chem.* **2016**, *7*, 2105.
 25. Tomita, H.; Sanda, F.; Endo, T. *J. Polym. Sci. Part A Polym. Chem.* **2001**, *39*, 860.
 26. Day, C. H. *Encycl. Toxicol.* **2005**, 420.
 27. Tomita, H.; Sanda, F.; Endo, T. *Macromolecules* **2001**, *34*, 727.
 28. Besse, V.; Foyer, G.; Auvergne, R.; Caillol, S.; Boutevin, B. *J. Polym. Sci. Part A Polym. Chem.* **2013**, *51*, 3284.
 29. Shaikh, A. A. G.; Sivaram, S. *Chem. Rev.* **1996**, *96*, 951.
 30. Matsuo, J.; Aoki, K.; Sanda, F.; Endo, T. *Macromolecules* **1998**, *31*, 4432.
 31. Zhao, W.; Liang, Z.; Feng, Z.; Xue, B.; Xiong, C.; Duan, C.; Ni, Y. *ACS Appl. Mater. Interfaces* **2021**, *13*, 28938.
 32. Maisonneuve, L.; Wirotius, A. L.; Alfos, C.; Grau, E.; Cramail, H. *Polym. Chem.* **2014**, *5*, 6142.
 33. Cramail, H.; Maisonneuve, L.; Grau, E.; Alfos, C. Six-membered cyclic biscarbonates **2013**, 1–30.
 34. Matsukizono, H.; Endo, T. *Polym. Chem.* **2016**, *7*, 958.
 35. Blattmann, H.; Lauth, M.; Mülhaupt, R. *Macromol. Mater. Eng.* **2016**, *301*, 944.
 36. Grignard, B.; Thomassin, J. M.; Gennen, S.; Poussard, L.; Bonnaud, L.; Raquez, J. M.; Dubois, P.; Tran, M. P.; Park, C. B.; Jerome, C.; Detrembleur, C. *Green Chem.* **2016**, *18*, 2206.
 37. Cornille, A.; Dworakowska, S.; Bogdal, D.; Boutevin, B.; Caillol, S. *Eur. Polym. J.* **2015**, *66*, 129.
 38. Clark, J. H.; Farmer, T. J.; Ingram, I. D. V.; Lie, Y.; North, M. *European J. Org. Chem.* **2018**, *2018*, 4265.
 39. Monie, F.; Grignard, B.; Thomassin, J. M.; Mereau, R.; Tassaing, T.; Jerome, C.; Detrembleur, C. *Angew. Chemie - Int. Ed.* **2020**, *59*, 17033.
 40. Coste, G.; Negrell, C.; Caillol, S. *Eur. Polym. J.* **2020**, *140*, 110029.
 41. Yang, G.; Rohde, B. J.; Tesefay, H.; Robertson, M. L. *ACS Sustain. Chem. Eng.* **2016**, *4*, 6524.
 42. Peyrton, J.; Avérous, L. *ACS Sustain. Chem. Eng.* **2021**, *9*, 4872.

43. Stefani, P. M.; Barchi, A. T.; Sabugal, J.; Vazquez, A. *J. Appl. Polym. Sci.* **2003**, *90*, 2992.
44. Tryznowski, M.; Żółek-Tryznowska, Z. *Materials (Basel)*. **2020**, *13*, 1.
45. Peyrton, J.; Avérous, L. *Mater. Sci. Eng. R Reports* **2021**, *145*.